Theor Chim Acta (1988) 74: 349-361

Theoretica Chimica Acta

Conjugated circuit theory for graphite*

G. E. Hite, T. P. Živković and D. J. Klein**

Department of Marine Sciences, Texas A&M University at Galveston, Galveston, TX 77553, USA

(Received December 9, 1987; revised and accepted February 2, 1988)

Computations for the "conjugated circuits" model which has previously only been treated for finite and quasi-one-dimensional conjugated π-networks are here extended to the graphite lattice. Many-body techniques give the resultant resonance energy per site as a function of a physically relevant long-range order parameter.

Key words: Resonance theory — Conjugated circuits — Valence-bond theory — Graphite — Many-body theory

1. Introduction

Valence-bond (VB) theory and various resonance-theoretic simplifications thereof have a long history [1] in chemistry. Especially its qualitative utilization and its correspondence with classical chemical-bonding ideas have been emphasized in the best-known works [2]. Quantitative computations even of a semiempirical nature have come only with some greater difficulty, especially for extended systems where the number of relevant VB structures increases exponentially with system size. Nevertheless nontrivial treatments of both quasi-one-dimensional [3, 4] and two-dimensional [3, 5] systems have been achieved most commonly just enumerating Kekulé structures. For the quasi-one-dimensional case extensions to compute Pauling bond orders [3] or conjugated-circuit counts [6, 7] have also been made, and for the two-dimensional case an extension to compute pair correlation functions [8] has been reported. Here we report an exact solution for the (resonance-theoretic) "conjugated-circuits" model of (Herndon [9] and Randić [10]) on a two-dimensional graphite lattice. In fact a whole family of solutions

---

* Research supported by The Welch Foundation of Houston, Texas

** *Permanent address*: Rugjer Bošković Institute, P.O.B. 1016, 41001 Zagreb, Yugoslavia is obtained, as a function of a physically relevant long-range order parameter [3, 6, 11] (or resonance quantum number).

The conjugated-circuits model is defined in terms of *Kekulé structures*, i.e., VB structures wherein every π-center is "paired" to exactly one other π-center. Given a Kekulé structure K a *conjugated circuit* is a cycle consisting of alternating single and double bonds (in K). For a "benzenoid" system, such as graphite, all conjugated circuits are [12] of size $4n+2$ (with n an integer), and the conjugated-circuits π-resonance energy for a system represented by the molecular *graph* G is [10]

$$E(G)=\sum_n R_n \sum_K N_{4n+2}(G,K)/\#(G), \tag{1.1}$$

where the sum is over Kekulé structures, $N_m(G,K)$ is the number of size-m conjugated circuits in the Kekulé structure K, and $\#(G)$ is the number of Kekulé structures in G. This model can be motivated in different ways [9, 10], and has proven very successful in several applications [6, 7, 9, 10, 13, 14]. Of particular note is the use of this model [14] in treating elemental conjugated carbon cages, such as the C_{60} "Buckminsterfullerene" structure recently proposed [15] as an especially stable component arising in molecular beam experiments. Indeed this proposal has contributed to a renewed interest in aromaticity concepts and in possible new [16] allotropic forms for carbon. A reason for interest in the many-body aspects of our work is the possible aid in treating high-temperature superconductors [17] within a recently proposed [18] "resonating valence-bond" description.

To carry out conjugated circuit calculations for a system G it is evident that a prerequisite is a Kekulé-structure count on G. Thence in Sect. 2 here we briefly review one such so-called transfer-matrix method [3] as applied to *poly-polyphenanthrene* strips of varying widths w. The $w=1$, $w=2$ and $w=3$ members of this family are indicated in Fig. 1. In Sect. 3 the transfer-matrix results are recast into a second-quantized language so as to allow the application of powerful many-body techniques. From this formulation we develop in Sect. 4 a "connection matrix" to solve in a formal manner the portion of the problem dealing with 6-circuits. Section 5 identifies the asymptotic $w \to \infty$ leading terms in this formal solution

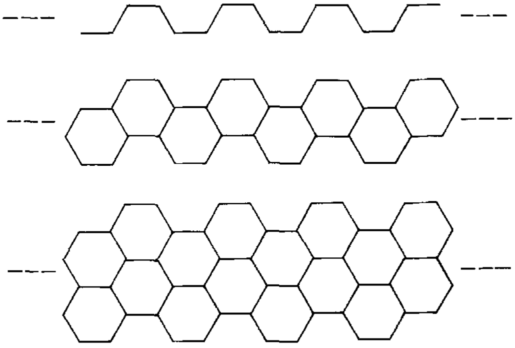

Fig. 1. The first 3 members of the poly-polyphenanthrene family of polymer strips

and presents them in a fairly explicit form. Section 6 treats two different portions of the 10-circuit contribution via the same technique. The analytic results of these Sects. 4–6 are given in terms of 3 by 3, 4 by 4, and 5 by 5 determinants whose matrix elements are certain types of k-space (i.e., wavevector-space) integrals. Numerical results are given in Sect. 7 and a discussion of the results is presented. If desired, most of this last section can be understood after reading through the first part of Sect. 2 dealing with the long-range order parameter.

2. Kekulé-structure count via transfer matrix

A Kekulé structure on a strip as in Fig. 1 may conveniently be described in terms of local structures specified at each location along the strip. Such a *local state* at a location as indicated by a vertical dashed line in Fig. 2 may be specified by a list of the positions of the various double bonds intersected by the vertical dashed line. Thence the possible bond positions are numbered from 1 to the strip width w, starting from the side with the "more exposed" position; this direction of numbering is indicated by arrows on the dashed lines of Fig. 2. A list of Q double-bond positions $m_1, m_2, \ldots, m_Q$ with $1 \leq m_1 < m_2 < \cdots < m_Q \leq w$ is abbreviated to $m(Q)$, and the associated local state is denoted $|m(Q)\rangle$. Then the local states proceeding form left to right in Fig. 2 are $|1,3\rangle$, $|1,2\rangle$, $|2,3\rangle$, $|1,2\rangle$, $|1,3\rangle$, $|1,3\rangle$, $|1,2\rangle$, $|2,3\rangle$.

A *transfer matrix* $\boldsymbol{T}$ counts the allowed ways to proceed from one local state to the next. That is, its element $\langle m'(Q')|\boldsymbol{T}|m(Q)\rangle$ is the number of ways of having local states $|m(Q)\rangle$ and $|m'(Q')\rangle$ at adjacent locations. It turns out [3] that $\boldsymbol{T}$ is block-diagonal with respect to Q, the number of horizontally oriented double bonds at each location along the strip. This block-diagonalization, which carries over to the Hamiltonian, identifies Q as a *resonance* quantum number. That a given Kekulé structure has the same Q down the whole length of a strip identifies Q as a *long-range order* parameter. Thence the number of Kekulé structures with a given value of Q is of interest and is denoted by $\#_Q(L)$. From the definition of the matrix elements of $\boldsymbol{T}$ it can be seen that $\langle m'(Q)|\boldsymbol{T}^d|m(Q)\rangle$ gives the number of ways of having local states $|m(Q)\rangle$ and $|m'(Q)\rangle$ at locations a distance d apart.

Generally, the Kekulé count will depend upon the nature of the ends of the strip, which in fact are usually consistent only with a certain value of Q. Focusing on bulk features here, we assume cyclic boundary conditions for a strip of even length L. Then

$$\#_Q(L) = \mathrm{Tr}_Q\, \boldsymbol{T}^L \tag{2.1}$$

where the trace is over the subspace labelled by Q.

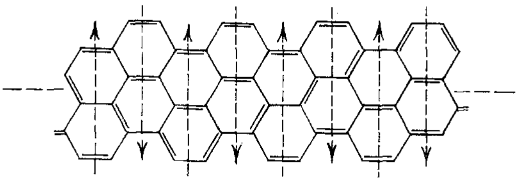

Fig. 2. A $Q=2$ sample Kekulé structure on a width $w=3$ strip

An eigenanalysis [3] for $\boldsymbol{T}$ is useful in refining the expression (2.1). As it turns out the eigenstates of $\boldsymbol{T}$ are labelled by sequences

$$k(Q) \equiv (k_1, k_2, \dots, k_Q), \text{ with } 1 \leq k_1 < k_2 < \cdots < k_Q \leq w \tag{2.2}$$

such that the associated eigenvalues of $\boldsymbol{T}$ are up to sign given by

$$\begin{aligned} \lambda_{k(Q)} &= \prod_{i=1}^{Q} \lambda_{k_i} \\ \lambda_k &= (-1)^{k+1} \Big/ \left\{ 2 \sin\left(\frac{2k-1}{2w+1} \frac{\pi}{2} \right) \right\}. \end{aligned} \tag{2.3}$$

The appropriate sign is just the parity of $i(Q/2)$, the integer part of $Q/2$, but it plays little role in the work here. The normalized eigenvector $|\lambda_{k(Q)}\rangle$ associated to $\lambda_{k(Q)}$ has components (on the $|m(Q)\rangle$ basis) each of which is a determinant of a matrix with (i, j)th element $\langle m_i | \lambda_{k_j} \rangle$,

$$\begin{aligned} \langle m(Q) | \lambda_{k(Q)} \rangle &= \det \langle m_i | \lambda_{k_j} \rangle \\ \langle m | \lambda_k \rangle &= \frac{2}{\sqrt{2w+1}} \sin\left(\frac{2k-1}{2w+1} m\pi \right), \; m, k = 1 \text{ to } w. \end{aligned} \tag{2.4}$$

Now (for even L) equation (2.1) may be recast as

$$\#_Q(L) = \sum_{k(Q)} \{\lambda_{k(Q)}\}^L. \tag{2.5}$$

For large L this is strongly dominated by the eigenvalue(s) of maximum magnitude. This unique eigenvalue is, up to sign, given by

$$\Lambda_Q = \prod_{k=1}^{Q} \lambda_k \tag{2.6}$$

and the associated eigenvector is denoted by $|\Lambda_Q\rangle$. Thence

$$\#_Q(L) \cong \Lambda_Q^L, \text{ as } L \to \infty. \tag{2.7}$$

From the simplest resonance theory [19] the most favored Q value would be that for which Λ_Q is a maximum, this occurring at $Q = i(w/3)$ or $Q = i(w/3) + 1$.

3. Second quantization

The results of the preceding section may be recast to reveal the potential for the use of powerful many-body techniques. First, the local-state space upon which $\boldsymbol{T}$ acts is [3] mathematically isomorphic to an antisymmetric *Fock space* with w *Fermionic orbitals*, each labelled by a potential double-bond position. Then we may introduce Fermionic *creation* and *annihilation* operators a_m^+ and a_m such that

$$\begin{aligned} \{a_m^+, a_n^+\} &= \{a_m, a_n\} = 0 \\ \{a_m^+, a_n\} &= \delta_{mn} \end{aligned} \tag{3.1}$$

and it is seen that $|m(Q)\rangle$ corresponds to a *Q-particle* Slater determinant with the orbitals labelled by $m_1, m_2, \dots, m_Q$ occupied,

$$|m(Q)\rangle = a_{m_1}^+ a_{m_2}^+ \cdots a_{m_Q}^+ |0\rangle, \tag{3.2}$$

where $|0\rangle$ is the *vacuum* state. It is to be emphasized that what we have are not conventional "orbitals" and "Q-particle" states and "vacuum" states, *but* rather a mathematical isomorphism to a structure to which such names are commonly applied. It is really the powerful and perfectly legitimate mathematical techniques associated to this language that we seek to use.

A second important point is that the eigenstates to $\boldsymbol{T}$ also correspond, within this isomorphism, to independent particle states

$$|\lambda_{k(Q)}\rangle = \alpha_{k_1}^+ \alpha_{k_2}^+ \cdots \alpha_{k_Q}^+ |0\rangle, \tag{3.3}$$

where α_k^+ and α_k are Fermionic creation and annihilation operators with

$$\alpha_k^+ = \sum_{m=1}^{w} \langle m|\lambda_k\rangle a_m^+. \tag{3.4}$$

The relation inverse to that of (3.4) is

$$a_m^+ = \sum_{k=1}^{w} \langle m|\lambda_k\rangle^* \alpha_k^+. \tag{3.5}$$

Now expectation values for such (independent-particle) eigenstates are susceptible to Wick's-theorem-type factorization. That is, it treats expectation values

$$\langle \Lambda_Q | b_1 b_2 \cdots b_{2n} | \Lambda_Q \rangle \equiv \langle b_1 b_2 \cdots b_{2n} \rangle, \tag{3.6}$$

where the b_i in our case are either purely creation operators or purely annihilation operators. Clearly for this expectation value to be nonzero there must be equal numbers of each. Thence let the n annihilation operators be A_i, $i=1$ to n, numbered as they appear in going from left to right in (3.6), and let the n creation operators be C_i, $i=1$ to n, numbered in going from right to left. Further define an n by n matrix $\boldsymbol{M}$ with (i,j)th element

$$\boldsymbol{M}_{ij} \equiv \begin{cases} +\langle C_i A_j \rangle, & C_i \text{ left of } A_j \text{ in (3.6)} \\ -\langle A_j C_i \rangle, & C_i \text{ right of } A_j \text{ in (3.6).} \end{cases} \tag{3.7}$$

Then the expectation value is given in terms of the determinant of $\boldsymbol{M}$

$$\langle b_1 b_2 \cdots b_{2n} \rangle = \pm \det \boldsymbol{M}, \tag{3.8}$$

where the sign here is given as the parity of the permutation carrying the A's and C's as they appear in the expectation value to the standard order $C_n \cdots C_2 C_1 A_1 A_2 \cdots A_n$. This Wick-type theorem of (3.8) is given in nearly this form by Linderberg and Öhrn [20]. (The temperature $1/\beta$ there is to be taken to 0, and their times may be used to specify an order for the operators, following which one takes the limit that all times approach 0.)

4. Counts for conjugated 6-circuits

A typical conjugated 6-circuit on a strip appears as in Fig. 3. There also are labelled several potential double-bond positions, where it is understood that the strip proceeds horizontally, as in Fig. 1. Now from Fig. 3 it is seen that this

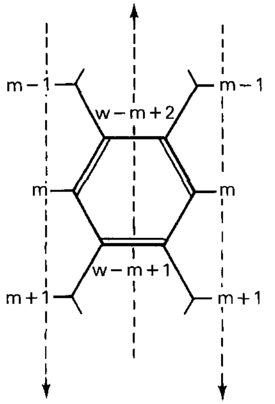

3

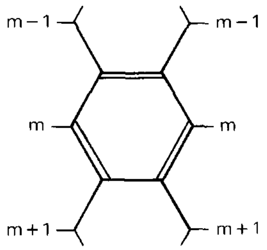

4

Fig. 3. The numbering of positions near a conjugated 6-circuit
Fig. 4. The conjugated 6-circuit "dual" to that of Fig. 3

particular conjugated circuit occurs if and only if: first, position m is "unoccupied" in the first column shown on the left; second, position $w-m+1$ is "occupied" in the next column; and third, position m is "unoccupied" in the third column, shown on the right. Then noting that $a_n a_n^+$ and $a_n^+ a_n$ are the projection operators for nonoccupation and occupation, respectively, of position n by a double bond, we obtain the number of Kekulé structures with this particular conjugated 6-circuit of Fig. 2 as

$$\mathrm{Tr}_Q \{a_m a_m^+ T a_{w-m+1}^+ a_{w-m+1} T a_m a_m^+ T^{L-2}\}. \tag{4.1}$$

Next, to every Kekulé structure with the conjugated 6-circuit of Fig. 2 there clearly corresponds exactly one Kekulé structure with the "dual" conjugated 6-circuit of Fig. 4; these two corresponding structures are the same except as regards this single circuit. Thus the count for these dual conjugated 6-circuits is the same and may be accounted for simply by multiplying the expression of (4.1) by 2. Further, summation over $m=2$ to w, yields the count for the whole column of 6-circuits at the given location along the strip, and multiplication by L accounts for the various locations. Thus the total conjugated 6-circuit count is

$$\#_Q^{(6)}(L) = 2L \sum_{m=2}^{w} \mathrm{Tr}_Q \{a_m a_m^+ T a_{w-m+1}^+ a_{w-m+1} T a_m a_m^+ T^{L-2}\}. \tag{4.2}$$

Just as in the argument leading to (2.7) we presently obtain

$$\#_Q^{(6)}(L) = 2L \sum_{m=2}^{w} \langle a_m a_m^+ T a_{w-m+1}^+ a_{w-m+1} T a_m a_m^+ \rangle \Lambda_Q^{L-2}, \; L \to \infty \tag{4.3}$$

where the notation for expectation values is as in (3.6). For the two operators remaining we may insert a spectral resolution, but the non-maximal eigenvalues cannot be neglected due to their size since they are not raised to a high power.

Thence with the utilization of this spectral resolution, with the introduction the decompositions of (3.5), and with the division by $\#_Q(L)$ as in (2.7), one obtains

$$\begin{aligned}\frac{\#_Q^{(6)}(L)}{\#_Q(L)}=\frac{2L}{\Lambda_Q^2}\sum_{m=2}^{w}\sum_{k'(Q)}\sum_{k''(Q)}\sum_{k_1k_2k_3k_4}&\{\langle m\,|\,\lambda_{k_1}\rangle\langle m\,|\,\lambda_{k_2}\rangle^*\langle m\,|\,\lambda_{k_3}\rangle\langle m\,|\,\lambda_{k_4}\rangle^*\\ &\times\langle\Lambda_Q\,|\,\alpha_{k_1}\alpha^+_{k_2}|\lambda_{k'(Q)}\rangle\lambda_{k'(Q)}\langle\lambda_{k'(Q)}|a^+_{w-m+1}a_{w-m+1}|\lambda_{k''(Q)}\rangle\\ &\times\lambda_{k''(Q)}\langle\lambda_{k''(Q)}|\alpha_{k_3}\alpha^+_{k_4}|\Lambda_Q\rangle\}.\end{aligned}\tag{4.4}$$

But the intermediate states labelled by $k'(Q)$ and $k''(Q)$ clearly yield a nonzero result only if they involve no more than the change of one orbital index from $k(Q)$ (since they are to be connected to $\langle\Lambda_Q|$ and $|\Lambda_Q\rangle$ on the left and right by a one-particle operator). More specifically we find that the only nonzero results occur for $\lambda_{k'(Q)}=\Lambda_Q\lambda_{k_1}/\lambda_{k_2}$ and $\lambda_{k''(Q)}=\Lambda_Q\lambda_{k_4}/\lambda_{k_3}$. Thence making this substitution and recognizing that the remaining $k'(Q)$ and $k''(Q)$ dependences appear simply as resolutions of the identity, one obtains

$$\begin{aligned}\frac{\#_Q^{(6)}(L)}{\#_Q(L)}=2L\sum_{m=2}^{w}\sum_{k_1k_2k_3k_4}&\left\{\prod_{i=1}^{4}\langle m|\lambda_{k_i}\rangle\right\}\\ &\times\langle\alpha_{k_1}\alpha^+_{k_2}a^+_{w-m+1}a_{w-m+1}\alpha_{k_3}\alpha^+_{k_4}\rangle\frac{\lambda_{k_1}\lambda_{k_4}}{\lambda_{k_2}\lambda_{k_3}}.\end{aligned}\tag{4.5}$$

Next introducing the operators

$$a_{m,i}\equiv\sum_{k}\lambda_k^i\langle m\,|\,\lambda_k\rangle\alpha_k\tag{4.6}$$

and their adjoints $a^+_{m,i}$, we obtain a compact expression for the *mean* conjugated 6-circuit count per site

$$\langle 6\rangle_{Q/w}\equiv\frac{\#_Q^{(6)}(L)}{2Lw\#_Q(L)}=\frac{1}{w}\sum_{m=2}^{w}\langle a_{m,1}a^+_{m,-1}a^+_{w-m+1}a_{w-m+1}a_{m,-1}a^+_{m,1}\rangle\tag{4.7}$$

valid in the limit of large L.

At this point the theorem of (3.8) may be applied to give

$$\langle 6\rangle_{Q/w}=-\frac{1}{w}\sum_{m=2}^{w}\det\begin{pmatrix}-\langle a_{m,1}a^+_{m,1}\rangle & -\langle a_{w-m+1}a^+_{w-m+1}\rangle & -\langle a_{m,-1}a^+_{m,1}\rangle\\ -\langle a_{m,1}a^+_{w-m+1}\rangle & \langle a^+_{w-m+1}a_{w-m+1}\rangle & \langle a^+_{w-m+1}a_{m,-1}\rangle\\ -\langle a_{m,1}a^+_{m,-1}\rangle & \langle a^+_{m,-1}a_{w-m+1}\rangle & \langle a^+_{m,-1}a_{m,-1}\rangle\end{pmatrix},\tag{4.8}$$

where also we have noted that $a_{m,0}=a_m$. There remains the evaluation of these single-particle expectation values in this determinant.

5. Matrix element evaluation

The matrix elements of the determinant in (4.8) and those of the following section are straightforward to evaluate for finite width strips. One of two generic forms they may take is

$$\begin{aligned}\langle a^{+}_{m,i}a_{n,j}\rangle &= \sum_{k,k'=1}^{w} \lambda^{i}_{k}\lambda^{j}_{k'}\langle m\,|\,\lambda_k\rangle\langle n\,|\,\lambda_{k'}\rangle^{*}\langle \alpha^{+}_{k}\alpha_{k'}\rangle \\ &= \sum_{k=1}^{Q} \lambda^{i+j}_{k}\langle m\,|\,\lambda_k\rangle\langle n\,|\,\lambda_k\rangle^{*}, \qquad (5.1)\end{aligned}$$

where we have noted (as follows from (3.3) and the discussion near (3.6)) that the first Q "eigenorbitals", with $k=1$ to Q, are "occupied" in $|\Lambda_Q\rangle$. The second generic form is

$$\langle a_{m,i}a^{+}_{n,j}\rangle = \sum_{k=Q+1}^{w} \lambda^{i+j}_{k}\langle m\,|\,\lambda_k\rangle\langle n\,|\,\lambda_k\rangle^{*}. \qquad (5.2)$$

For finite w these are finite sums with the summands given explicitly in (2.3) and (2.4). Thence the finite-width (infinite length) result is expressed as a finite calculation, though tedious and hence conveniently carried out by computer.

For the infinite-width limit the computation may be simplified. The development treats two cases dependent upon the relation between m and n: either $n=m+\delta$ or $n=w-m+\delta$ with δ a small integer $0, \pm 1, \pm 2$. In the first case, the m-dependent portion of the summands in (5.1) and (5.2) may be rewritten as

$$\begin{aligned}\langle m\,|\,\lambda_k\rangle\langle m+\delta\,|\,\lambda_k\rangle^{*} &= \frac{4}{2w+1}\sin\theta m\cdot\sin\theta(m+\delta) \\ &= \frac{2}{w+1}\{\cos\delta\theta-\cos\,(2m+\delta)\theta\}, \qquad (5.3)\end{aligned}$$

where for brevity $\theta\equiv(2k-1)\pi/(2w+1)$. In the second case the corresponding quantity is rewritten as

$$\begin{aligned}\langle m\,|\,\lambda_k\rangle\langle w-m+\delta\,|\,\lambda_k\rangle^{*} &= \frac{2}{2w+1}\{\cos\,(2m-w-\delta)\theta-\cos\,(w+\delta)\theta\} \\ &= \frac{2}{2w+1}(-1)^{k+1}\{\sin\,(2m-\delta+\tfrac{1}{2})\theta+\sin\,(\delta-\tfrac{1}{2})\theta\} \qquad (5.4)\end{aligned}$$

Now for typical values of m and k, the m-dependent terms in the resulting expressions of (5.3) and (5.4) will lead to negligible summations, because these terms will oscillate in sign as k varies while the λ^{i+j}_{k} remaining in the summands will vary much more slowly—infinitely more slowly in the $w\to\infty$ limit. One way to see the negligible contribution of these terms more clearly is to replace the k-sums by integrals over θ. Thence one finds the matrix elements of the type that arise take only either the form

$$\frac{1}{\pi}\int\left\{\sin\frac{\theta}{2}\right\}^{-i-j}\{\cos\delta\theta-\cos\,(2m+\delta)\theta\}\,d\theta \qquad (5.5)$$

when $n=m+\delta$ and also $i+j=\text{even}$, or

$$\frac{1}{\pi}\int\left\{\sin\frac{\theta}{2}\right\}^{-i-j}\{\sin(\delta-\tfrac{1}{2})\theta+\sin(2m-\delta+\tfrac{1}{2})\theta\}\,d\theta \tag{5.6}$$

when $n=w-m+\delta$ and also $i+j=\text{odd}$. The ranges of integration are 0 to $q\pi$ for the integrals associated to (5.1) and $q\pi$ to π for (5.2), where q is a "normalized" resonance quantum number

$$q\equiv Q/w \tag{5.7}$$

which in fact is just the double-bond density on the horizontally-oriented bond positions. Then for $w\to\infty$, most $m\to\infty$ too, and (5.5) and (5.6) take the forms

$$-\frac{1}{\pi}\int\cos d\theta\cdot\left\{\sin\frac{\theta}{2}\right\}^{-i-j}d\theta \quad\text{and}\quad \frac{1}{\pi}\int\sin(\delta-\tfrac{1}{2})\theta\cdot\left\{\sin\frac{\theta}{2}\right\}^{-i-j}d\theta \tag{5.8}$$

which are analytically integrable by standard means. Thence (4.8) is finally obtained as

$$\langle 6\rangle_q=-\det\begin{pmatrix} -\frac{1}{2\pi}\cot q\frac{\pi}{2} & \frac{1}{2}(q-1) & q-1\\ \frac{1}{2}(q-1) & q & -q+\frac{1}{\pi}\sin q\pi\\ q-1 & -q+\frac{1}{\pi}\sin q\pi & 2q-\frac{2}{\pi}\sin q\pi \end{pmatrix}, \tag{5.9}$$

which in fact is exact (in the large L and w limit) except for corrections of order $1/w$ and higher.

6. Conjugated 10-circuits

Of the two types of orientations possible for a conjugated 10-circuit, we first treat the "diagonal" orientation of Fig. 5. There also we have labelled several potential double-bond positions, with the strip proceeding horizontally. Now it is seen that the particular conjugated circuit occurs if and only if: first, position m is

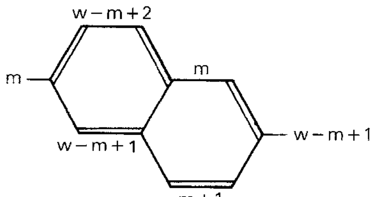

5

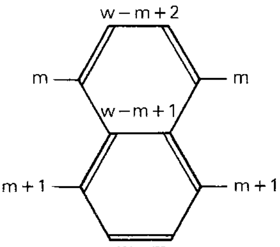

6

Fig. 5. The numbering of the positions near a "downward" diagonally-oriented conjugated 10-circuit

Fig. 6. The numbering around a vertically oriented conjugated 10-circuit

"unoccupied" in the first column; second, position $w-m+1$ is "occupied" in the second column; third, position $m+1$ is "occupied" in the third column; and fourth, position $w-m+1$ is "unoccupied" in the fourth column. Thus, following the argument leading to (4.2), we obtain the total count for like-oriented diagonal conjugated 10-circuits

$$\#_Q^{(10)d}(L) = 2L \sum_{m=2}^{w} \mathrm{Tr}_Q$$

$$\{a_m a_m^+ T a_{w-m+1}^+ a_{w-m+1} T a_{m+1}^+ a_{m+1} T a_{w-m+1} a_{w-m+1}^+ T^{L-3}\}. \tag{6.1}$$

The type of argument leading to (4.5) and (4.7) now can be repeated for the present case to give

$$\langle 10, d\rangle_q \equiv \frac{\#_Q^{(10)d}(L)}{2Lw\#_Q(L)} = \frac{1}{w\Lambda_Q} \sum_{m=2}^{w} \sum_{k''(Q)} \{\langle \Lambda_Q | a_{m,1} a_{m,-1}^+ a_{w-m+1}^+ a_{w-m+1} | \lambda_{k''(Q)}\rangle$$

$$\times \lambda_{k''(Q)} \langle \lambda_{k''(Q)} | a_{m+1}^+ a_{m+1} a_{w-m+1,1} a_{w-m+1,1}^+ | \Lambda_Q\rangle. \tag{6.2}$$

But here too the $|k''(Q)\rangle$ that give nonzero contributions cannot differ too greatly from $|\Lambda_Q\rangle$. That is, in the last matrix element here the a^+'s and a's can be resolved into α^+'s and α's, then $\lambda_{k''(Q)}$ replaced by Λ_Q times an adjustment factor with two ratios of λ_k's, and thence the resolution of the identity recognized and resummed to give a mean diagonal conjugated 10-circuit count

$$\langle 10, d\rangle_Q = \frac{1}{w} \sum_{m=2}^{w} \langle a_{m,1} a_{m,-1}^+ a_{w-m+1}^+ a_{w-m+1} a_{m+1,1}^+ a_{m+1,-1} a_{w-m+1,-2} a_{w-m+1,2}^+\rangle. \tag{6.3}$$

Finally the theorem of (3.8) is used to yield a determinamental formula and then the methods of Sect. 5 are used to evaluate the matrix elements, so that

$$\langle 10, d\rangle_q = \det \begin{pmatrix} \frac{1}{2}c & -c & \frac{1}{2}(q-1) & q-1 \\ -c+\frac{1}{2}(1-q) & \frac{1}{2}(q-1) & q & q-s_1 \\ \frac{1}{2}(q-1) & q & q-s_1 & 2(q-s_1) \\ q-1 & s_1-q & 2s_1-s_2-q & 4s_1-s_2-3q \end{pmatrix} \tag{6.4}$$

where abbreviations for several simple trigonometric functions have been introduced

$$c \equiv \frac{1}{2\pi} \cot \frac{\pi}{2} q$$

$$s_p \equiv \frac{1}{p\pi} \sin p\pi q. \tag{6.5}$$

Again though (6.3) is exact, the suppression of the m-dependence leads to a result in (6.4) that is only exact disregarding corrections of order $1/w$ and higher.

The second "vertical" type of orientation for conjugated 10-circuits is illustrated in Fig. 6, with labelled potential double-bond positions. This particular conjugated circuit occurs if and only if: first, positions m and $m+1$ are "unoccupied" in the first column; second, position $w-m$ is "occupied" in the second column; and third, positions m and $m+1$ are again "unoccupied" in the third column. Then following the now familiar arguments we obtain the mean vertical conjugated 10-circuit count as

$$\langle 10, v\rangle_q = \det\begin{pmatrix} -c & -c+\tfrac{1}{2}(1-q) & \tfrac{1}{2}(1-q) & s_1 & q-1 \\ -c+\tfrac{1}{2}(1-q) & -c & -s_1+\tfrac{1}{2}(1-q) & q-1 & s_1 \\ \tfrac{1}{2}(1-q) & -s_1+\tfrac{1}{2}(1-q) & q & -s_1+s_2 & s_1-q \\ s_1 & q-1 & -s_1+s_2 & 2(q-s_1) & 2s_1-s_2-q \\ q-1 & s_1 & s_1-q & 2s_1-s_2-q & 2(q-s_1) \end{pmatrix} \tag{6.6}$$

again exact up to order $1/w$.

The total mean conjugated 10-circuit count then is

$$\langle 10\rangle_q = 2\langle 10, d\rangle_q + \langle 10, v\rangle_q, \tag{6.7}$$

where the factor of 2 arises for $\langle 10, d\rangle_q$ because there are two possible orientations, downward slanted as in Fig. 5 and also upward slanted. Of course for finite w, $\langle 10\rangle_q$ could be precisely evaluated, as a finite sum over determinants as in (6.5) and (6.6) but with matrix elements expressed as finite sums as in (5.1) and (5.2).

7. Results and discussion

The final resonance energy per site

$$\text{R.E.}(q) = R_1\langle 6\rangle_q + R_2\langle 10\rangle_q \tag{7.1}$$

is a function of the "normalized" resonance quantum number $q \equiv Q/w$, giving the fraction of bonds oriented in one direction, each fraction q identifying a class of Kekulé structures. Explicit asymptotically exact expressions for the mean (per site) conjugated 6- and 10-circuit counts are given by (5.9), (6.4), (6.5) and (6.6). Evaluation of these expressions for the 6-circuit density, for the vertically-oriented 10-circuit density, and for either diagonally-oriented 10-circuit density yields the curves for $\langle 6\rangle_q$, $\langle 10, v\rangle_q$, and $\langle 10, d\rangle_q$ shown in Fig. 7. Using these results one

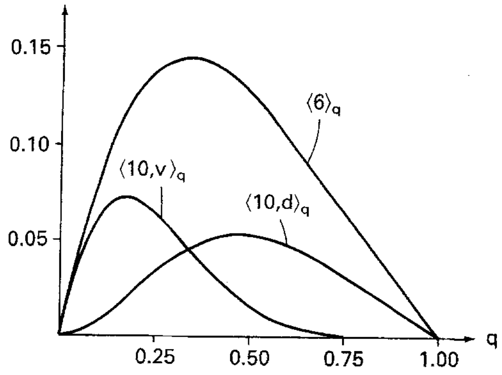

Fig. 7. The three different conjugated-circuit counts described in the text

may compute the resonance energy per site via (6.6) and (7.1), if a choice for the parameters R_1 and R_2 is made, such as that recommended by Herndon [9]

$$R_1 = 0.841 \text{ eV} \quad \text{and} \quad R_2 = 0.336 \text{ eV}. \tag{7.2}$$

Alternative parameterizations [10] were not used since they assume conjugated 14-circuit counts, which we have not made here. (By our present approach these counts for graphite would involve four additional determinants of sizes up to 7 by 7.)

Our overall resonance energy per site referenced against the (maximum) value (of $0.1996\,R_1$) at $q = 1/3$ is shown in the solid curve of Fig. 8 where also we show in the dashed curve the result for a simple Kekulé-structure estimator of the resonance energy. This estimator [9] is proportional to the logarithm of the number of Kekulé structures as previously obtained [3] and as here referenced against its (maximum) value (of 0.161533) at $q = 1/3$. It appears that the maximum for the Herndon–Simpson resonance energy also occurs at $q = 1/3$, and evidently so also do the maxima for $\langle 6\rangle_q$ and $\langle 10\rangle_q$. Thence the values of the various expectation values at $q = 1/3$ are of interest

$$\begin{aligned} \langle 6\rangle_{1/3} &= 0.1450142 \\ \langle 10, d\rangle_{1/3} &= 0.4556076 \\ \langle 10, v\rangle_{1/3} &= \langle 10, d\rangle_{1/3}. \end{aligned} \tag{7.3}$$

Since the resonance energy maxima occur at $q = 1/3$, one finds that: these models do not require [11, 21] a distortion from hexagonal symmetry; the Pauling π-bond-order of every bond is the same (1/3) in the most stable phase of the extended honeycomb lattice, and all bond lengths are equal. Though these results are as many expect, it is of interest to verify them for the conjugated-circuit model, especially since there has been some experimental [22] ambiguity. Similar conclusions evidently apply [23] for the Hückel molecular orbital model for graphite. Finally our results here provide the *first* asymptotically exact conjugated-circuit counts for a two-dimensionally extended network.

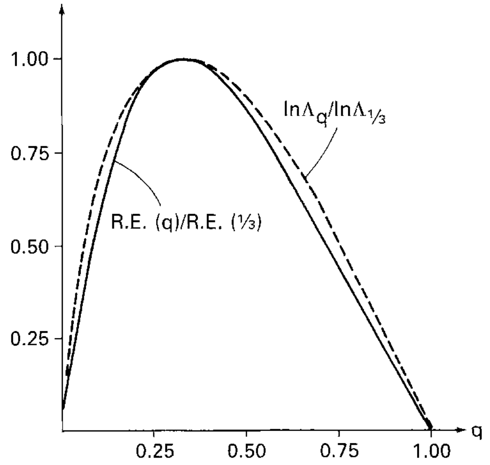

Fig. 8. Two different resonance-energy estimates as a function of the fraction q of double bonds oriented "longitudinally"

References

1. See, e.g. Klein DJ, Trinajstić N (1988) Valence bond theory and chemical structure. Elsevier, Amsterdam
2. See, e.g. (a) Pauling L (1939) The nature of the chemical bond. Cornell University Press, Ithaca, New York; (b) Wheland GW (1955) Resonance in organic chemistry. Wiley, New York
3. Klein DJ, Hite GE, Seitz WA, Schmalz TG (1986) Theor Chim Acta 69:409-423
4. See a couple dozen references in [3] and also (a) Herndon WC (1973) Tetrahedron 29:3; (b) Ahrens JH (1981) J Comb Theory A31:277; (c) Knop JV, Szymanski K, Trinajstić N, Krivka P (1984) Comp & Math with Appls 10:369; (d) Cyvin SJ, Gutman I (1985) J Serbian Chem Soc 50:443; (e) Stanley RP (1985) Discuss Appl Math 12:81; (f) Cyvin SJ (1985) Monatsh Chem 117:33; (g) Cyvin SJ, Cyvin BN, Gutman I (1985) Z Naturforsch 40a:1253; (h) Cyvin SJ, Gutman I (1986) Z Naturforsch 41a:1079; (i) He W, He W (1986) Theor Chim Acta 70:43; (j) He W, He W (submitted 1987) Theor Chim Acta; (k) Cyvin SJ, Cyvin BN, Chen RS (1987) Match 22:151
5. See several references in [3] and also (a) Bhattacharjee SM, Nagle JF (1985) Phys Rev A31:3199; (b) Cyvin SJ (1986) Monatsh Chem 117:33; (c) Nagle JF, Yokoi CSO (1987) Phys Rev B 35:5307
6. Klein DJ, Hite GE, Schmalz TG (1986) J Comput Chem 7:443
7. (a) Randić M (1980) Int J Quantum Chem 17:549; (b) Randić M, Gimarc BM, Trinajstić N (1986) Croat Chem Acta 59:345; (c) Seitz WA, Hite GE, Schmalz TG, Klein DJ (1987). In: King RB, Rouvray DH (eds) Graph theory and topology in chemistry. Elsevier, Amsterdam, p 458; (d) Seitz WA, Schmalz TG in [1]
8. Yokoi CSO, Nagle JF, Salinas SR (1986) J Stat Phys 44:729
9. (a)Herndon WC (1983) J Am Chem Soc 95:2404; (b) Herndon WC, Ellzey Jr ML (1974) J Am Chem Soc 96:6631
10. (a) Randić M (1976) Chem Phys Lett 38:68; (b) Randić M (1977) J Am Chem Soc 99:444; (c) Randić M, Nikolić S, Trinajstić N (1987). In: King RB, Rouvray DH (ed) Graph theory and topology in chemistry. Elsevier, Amsterdam, p 429
11. Klein DJ (1979) Int J Quantum Chem 13S:294
12. Cvetković D, Gutman I, Trinajstić N (1974) J Chem Phys 61:2700
13. See, e.g. (a) Randić M (1977) Tetrahedron 33:1905; (b) Herndon WC (1981) J Org Chem 46:2119; (c) Herndon WC (1983) J Molec Struct 103:219; (d) Randić M, Trinajstić N (1984) J Am Chem Soc 106:4428; (e) Randić M, Trinajstić N, Knop, JV, Jericević Z (1985) J Am Chem Soc 107:849
14. (a) Klein DJ, Schmalz TG, Seitz WA, Hite GE (1986) J Am Chem Soc 108:1301; (b) Schmalz TG, Klein DJ, Seitz WA, Hite GE (1986) Chem Phys Lett 130:203; (c) Klein DJ, Schmalz TG, Seitz WA (1986) Nature 323:703; (d) Schmalz TG, Seitz WA, Klein DJ, Hite GE (1988) J Am Chem Soc 110:1113
15. (a) Kroto HW, Heath JR, O'Brien SC, Curl RF, Smalley RE (1985) Nature 318:162; (b) Heath JR, O'Brien SC, Curl RF, Kroto HW, Smalley RE (1988) Acc Chem Res (in press)
16. See, e.g. (a) Merz Jr KM, Hoffmann R, Balaban AT (1987) J Am Chem Soc 109:6742; (b) Baughman RH, Eckhardt H, Kertesz M (1987) J Chem Phys 87:6687
17. See, e.g. (a) Bednorz JG, Müller KA (1986) Z Phys B64:189; (b) Wu MK, Ashburn JR, Torng CT, Hos PH, Meng RL, Gas L, Huang ZJ, Wang YQ, Chu CW (1987) Phys Rev Lett 58:908; (c) Bednorz JG, Müller KA (1987) Science 237:1133
18. (a) Anderson PW (1987) Science 235:1196; (b) Anderson PW, Baskaran G, Zou Z, Hsu T (1987) Phys Rev Lett 58:2790; (c) Pauling L (1987) Phys Rev Lett 59:225; (d) Hirsch JE (1987) Phys Rev B35:8726; (e) Kivelson SA, Rokshar DS, Sethna JP (1987) Phys Rev B35:8865; (f) Affleck J, Kennedy T, Lieb EH, Tasaki H (1987) Phys Rev Lett 59:799; (g) Messmer RP (1987) Solid State Commun 63:405; (h) Schipper PE (1987) Chem Phys Lett 142:393
19. (a) Carter PG (1949) Trans Faraday Soc 45:497; (b) Swinborne-Sheldrake R, Herndon WC, Gutman I (1975) Tetrahedron Lett 1975:755; (c) Seitz WA, Klein DJ, Schmalz TG, Garcia-Bach MA (1985) Chem Phys Lett 115:139
20. Linderberg J, Öhrn Y (1973) Propagators in quantum chemistry. Academic Press, New York, appendix to chap 11
21. Pauling L (1966) Proc Natl Acad Sci 56:1646
22. Lukesh JS (1950) Phys Rev 80:226; Lukesh JS (1951) Phys Rev 84:1068
23. Anno T, Coulson CA (1961) Proc Roy Soc London A254:165